Optical and Quantum Electronics (2018) 50:342
https://doi.org/10.1007/s11082-018-1606-x

Theoretical investigation of hot electron cooling process in GaAs/AlAs cylindrical quantum wire under the influence of an intense electromagnetic wave

Khang D. Pham[1,2] · **Chuong V. Nguyen**[3] · **Nguyen N. Hieu**[4] · **Huynh V. Phuc**[5] · **Bui D. Hoi**[6] · **Bui M. H. Hoa**[6] · **Le T. T. Phuong**[6]

Received: 18 March 2018 / Accepted: 21 August 2018

Abstract

Hot electrons cooling by phonons in GaAs/AlAs cylindrical quantum wire (CQW), under the influence of an intense electromagnetic wave (EMW), is studied theoretically. Analytic expression for the electron cooling power (CP) is derived from the quantum transport equation for phonons, using the Hamiltonian of interacting electron–optical phonon system. Both photon absorption and emission processes are considered. Numerical results show that the CP reaches maximum when the energy difference between electronic subbands equals the energy of an optical phonon plus the photon energy. Under the influence of the EMW, the negative CP is observed showing that electrons gain energy from phonon and photon instead of losing their energy. Also, the CP increases with increasing the EMW amplitude. Our results theoretically clarify the mechanism of the electron cooling process by phonons in the GaAs/AlAs CQW under the EMW, which is of significance for designing and fabricating high-speed nanoelectronic devices based on this material.

Keywords Hot electron cooling · Cooling power · Quantum wire · Electron–phonon interaction

✉ Le T. T. Phuong
thuphuonghueuni@gmail.com

Khang D. Pham
phamdinhkhang@tdt.edu.vn

Bui D. Hoi
buidinhhoi@hueuni.edu.vn

1 Theoretical Physics Research Group, Advanced Institute of Materials Science, Ton Duc Thang University, Ho Chi Minh City, Vietnam

2 Faculty of Applied Sciences, Ton Duc Thang University, Ho Chi Minh City, Vietnam

3 Department of Materials Science and Engineering, Le Quy Don Technical University, Ha Noi, Vietnam

4 Institute of Research and Development, Duy Tan University, 03 Quang Trung, Da Nang, Vietnam

5 Division of Theoretical Physics, Dong Thap University, Cao Lanh, Dong Thap, Vietnam

6 Center for Theoretical and Computational Physics, University of Education, Hue University, Hue, Vietnam

Published online: 27 August 2018

1 Introduction

It is well-known that in a crystalline solid, the excitation of electrons into subbands results in their non-equilibrium distribution function and makes their temperature different from the lattice temperature. The non-equilibrium distribution function is thermalised rapidly to the Fermi function with a high electron temperature. The thermalisation process takes place very quickly (in about tens of femtoseconds) via electron–electron scattering in which the energy transferred to lattice by electrons is negligible so that the electron temperature remains greater than the lattice temperature, T_L (Balkan 1998; Lee et al. 1995). It then leads to the formation of "hot electron" temperature (T_e) (Bhargavi and Kubakaddi 2016). In the steady state, hot electrons lose their energy by emission of acoustic phonon at low temperature and of optical phonons at higher temperature. This process is referred as hot electron cooling by phonons. The mechanisms of electron cooling can be extracted, in principle, from the dependence of the hot electron relaxation on the temperature and carrier density (Kaasbjerg et al. 2014). Also, in pure samples electron scattering by phonons sets the ultimate limit on its intrinsic mobility, which plays important role for applications in high speed devices (Kubakaddi 2016). Hot electron energy loss rate by phonon emission is another property which significantly affects the device operation under high field conditions.

On the other hand, in low-dimensional materials, the confinement of carriers results in many exceptional physical features, including electron–phonon interaction in comparison to bulk materials (Stroscio and Dutta 2001). In particular, for novel 2D materials such as graphene and other atomically layered materials (Castro Neto et al. 2009; Das Sarma et al. 2011; Butler 2013; Gupta et al. 2015; Iacopi et al. 2016; Sangwan and Hersam 2018), the electron–phonon interaction shows many exotic behaviors. The effect of electron–phonon interaction on many effects in those materials has been also investigated in details (Yarmohammadi 2016; Kubakaddi 2009; Xu et al. 2010; Mori and Ando 2011; Yarmohammadi 2017a; Nguyen 2017; Yarmohammadi et al. 2017; Hoi et al. 2018; Yarmohammadi 2017b). In general, the hot electron cooling by phonons has been studied both theoretically and experimentally not only in conventional two-dimensional semiconductor heterostructures (Kubakaddi et al. 2003; Ma et al. 1991; Xu 1996; Fletcher et al. 1997; Qu et al. 2005; Sippel 2015), but also in advanced single-layer 2D materials such as graphene (Betz 2012; Bhargavi and Kubakaddi 2014; Stange et al. 2015; Kubakaddi 2018), monolayer MoS_2 and other transition metal dichalcogenides monolayers Kaasbjerg et al. (2014), and three dimensional Dirac fermion systems (Bhargavi and Kubakaddi 2016). For one-dimensional quantum wires, there have been also some studies on the hot electron relaxation dynamics carried out by R. Gaka and co-workers using Monte Carlo simulations (Gaška et al. 1994; Mitin et al. 1994; Gaška et al. 1994). However, experimental and theoretical studies on this problem in quantum wires have not attracted much attention so far, especially in the presence of an electromagnetic wave (EMW).

In the present work, we investigate the hot electrons cooling process in the GaAs/AlAs cylindrical quantum wire (CQW) in the presence of an intense EMW. The cooling power or electron energy loss rate is calculated by assuming that optical phonons emission is the source of electrons cooling. The paper is organised as follows. In Sect. 2, we introduce the theoretical model and brief derivation of a quantum transport equation for the average number of phonons. In Sect. 3, the expression for the CP is derived. Numerical results and discussion are given in Sect. 4. Finally, concluding remarks are listed in Sect. 5.

2 Theoretical model and quantum transport equation for phonons

We are interested in modelling a cylindrical GaAs quantum wire of radius R and length L ($L \gg R$) embedded in AlAs. Under the infinitely deep confinement potential approximation, the electron wave function can be written as (Wang and Lei 1994)

$$\psi_{\ell,j,k_z}(\mathbf{r}) = \frac{\mathrm{e}^{\mathrm{i}k_z z}}{\sqrt{L}} D_{\ell,j} J_\ell\left(x_{\ell,j}\frac{r}{R}\right)\mathrm{e}^{i\ell\phi}, \tag{1}$$

with the corresponding energy

$$E_{n,\ell}(k_z) = \frac{\hbar^2 k_z^2}{2m_\mathrm{e}} + \frac{\hbar^2 (x_{n,\ell})^2}{2m_\mathrm{e}R^2}, \tag{2}$$

where $n = 0, \pm 1, \pm 2, \ldots$ is the azimuthal quantum number; $\ell = 1, 2, 3, \ldots$ is the radial quantum number; $\mathbf{r} = (r, \phi, z)$ are the cylindrical coordinates for the system and k_z denotes the axial wave-vector component. $D_{n,\ell} = 1/(\sqrt{\pi} y_{n,\ell} R)$ is the normalisation factor; $x_{n,\ell}$ is the ℓth zero of the nth order Bessel function, i.e., $J_n(x_{n,\ell}) = 0$ and $y_{n,\ell} = J_{n+1}(x_{n,\ell})$; and m_e is the effective mass of electron.

When the electron density in the wire is small enough and the temperature is low enough ($k_\mathrm{B}T_\mathrm{e} \ll \varDelta E$ where $\varDelta E$ is the energy difference between the ground and first-excited states), only the lowest subband is occupied. For the quantum wire with the only one occupied subband, the scattering rate is determined by intra-subband electron–phonon interaction via the continuous Frohlich Hamiltonian (Shadrin et al. 1994). The Hamiltonian of the electron–phonon system in the presence of an intense EMW can be written in the secondary quantisation representation as $H = H_0 + U$, in which Kang et al. (2004)

$$H_0 = \sum_{n,\ell,k_z} E_{n,\ell}\left(\mathbf{k}_z - \frac{e}{\hbar c}\mathbf{A}(t)\right) a^+_{n,\ell,k_z} a_{n,\ell,k_z} + \sum_{\mathbf{q}} \hbar\omega_{\mathbf{q}} b^+_{\mathbf{q}} b_{\mathbf{q}}, \tag{3}$$

$$U = \sum_{n,n',\ell,\ell'} \sum_{k_z,\mathbf{q}} C_{\mathbf{q}} M_{n,\ell,n',\ell'}(q_\perp) a^+_{n',\ell',k_z+q_z} a_{n,\ell,k_z} (b_{\mathbf{q}} + b^+_{-\mathbf{q}}), \tag{4}$$

where $|n, \ell, k_z\rangle$ and $|n', \ell', k_z + q_z\rangle$ are electron states before and after scattering; a^+_{n,ℓ,k_z} and a_{n,ℓ,k_z} ($b^+_{\mathbf{q}}$ and $b_{\mathbf{q}}$) denote the creation and annihilation operators of electron (phonon) respectively; $\mathbf{q} = (q_x, q_y, q_z)$ is the phonon wave vector; $\mathbf{A}(t)$ is the vector potential of the EMW which is given, for a linear polarised EMW, by $\mathbf{A}(t) = (e/\varOmega)\mathbf{E}_0 \sin \varOmega t$ where e, E_0, and $\varOmega$ are, respectively, the electron charge, the EMW amplitude, and the EMW frequency; $\hbar\omega_{\mathbf{q}}$ is the phonon energy with the wave vector $\mathbf{q}$; $C_{\mathbf{q}}$ is the electron–phonon coupling factor which depends on the scattering mechanism; and the matrix element $M_{n,\ell,n',\ell'}(q_\perp)$ which characterises the configuration of electron confinement in the CQW takes the form (Masale and Constantinou 1993)

$$M_{n,\ell,n',\ell'}(y) = \int_0^1 x J_{|n-n'|}(yx) \psi^*_{n',\ell'}(x) \psi_{n,\ell}(x) dx, \tag{5}$$

where $y = q_\perp R$, $q_\perp = \sqrt{q_x^2 + q_y^2}$.

In order to establish a quantum transport equation for phonons in the CQW, we use the general quantum equation for the particle number operator $N_{\mathbf{q}} = \left\langle b^+_{\mathbf{q}} b_{\mathbf{q}} \right\rangle_t$

$$i\hbar \frac{N_{\mathbf{q}}(t)}{\partial t} = \left\langle [b^+_{\mathbf{q}} b_{\mathbf{q}}, H] \right\rangle_t, \tag{6}$$

where $\langle ... \rangle_t$ denotes a statistical average value at the moment t. Using the Hamiltonian H and usual commutation relations of the creation and annihilation operators, after some manipulations we obtain

$$\begin{aligned}
\frac{\partial N_{\mathbf{q}}(t)}{\partial t} =& \frac{\pi}{\hbar} \sum_{n,\ell,n',\ell',k_z} |C_{\mathbf{q}}|^2 |M_{n,\ell,n',\ell'}(\mathbf{q})|^2 \sum_{s=-\infty}^{+\infty} J_s^2\left(\frac{\Lambda}{\hbar\Omega}\right) \\
& \times \Big\{ \Big[(1+N_{\mathbf{q}}) f_{n',\ell',k_z+q_z}\left(1 - f_{n,\ell,k_z}\right) - N_{\mathbf{q}} f_{n,\ell,k_z}\left(1 - f_{n,\ell,k_z+q_z}\right) \Big] \\
& \times \delta\Big(E_{n,\ell}(k_z) - E_{n',\ell'}(k_z + q_z) + \hbar\omega_{\mathbf{q}} + s\hbar\Omega \Big) \\
& - \Big[N_{\mathbf{q}} f_{n',\ell',k_z-q_z}\left(1 - f_{n,\ell,k_z}\right) - (1+N_{\mathbf{q}}) f_{n,\ell,k_z}\left(1 - f_{n,\ell,k_z-q_z}\right) \Big] \\
& \times \delta\Big(E_{n,\ell}(k_z) - E_{n',\ell'}(k_z - q_z) - \hbar\omega_{\mathbf{q}} - s\hbar\Omega \Big) \Big\},
\end{aligned} \tag{7}$$

where $\Lambda = e\hbar\mathbf{q}\mathbf{E}_0/(m_e\Omega)$ is the field parameter; $N_{\mathbf{q}}$ and f_{n,ℓ,k_z} are, respectively, the phonon and the electron distributions with lattice (phonon) temperature T_L and electron temperature T_e, the index s represents the processes of s photon absorption (emission) when $s > 0$ ($s < 0$). The terms in the square brackets correspond to the absorption and the emission processes of a phonon with energy $\hbar\omega_{\mathbf{q}}$ by the hot electron distribution. For phonons in equilibrium with a phonon bath at temperature T, i.e., $T_L = T$, the phonon distribution is given by the Bose–Einstein distribution (Kaasbjerg et al. 2014).

3 General analytic expression for the hot electrons cooling power in CQW

We now calculate the electron cooling power (P) by assuming that electrons loss their energy to phonons only. The electron cooling power is defined as the rate at which the hot electron distribution loses its energy to the phonons system. As this is equivalent to the rate of change of the energy residing in the phonons, the cooling power can be obtained as Smith and Jensen (1989)

$$P = \sum_{\mathbf{q}} \hbar\omega_{\mathbf{q}} \left(\frac{\partial N_{\mathbf{q}}}{\partial t} \right), \tag{8}$$

where $\left(\partial N_{\mathbf{q}}/\partial t\right)$ is the collision integral which gives the rate of change of the phonon distribution function $N_{\mathbf{q}}$ due to electron–phonon scattering which has been derived in the previous section.

Inserting Eqs. (7) into (8) then using the identities $f_k(1-f_{k+q})N_q = f_{k+q}(1-f_k)(1+N_q)$ and $f_{k+q}(1-f_k) = N_q(f_k - f_{k+q})$, the cooling power will be recast as

$$P = F(T_e) - F(T), \tag{9}$$

where

$$\begin{aligned} F(T) = &\frac{\pi}{\hbar} \sum_{n,\ell,n',\ell'} \sum_{k_z,\mathbf{q}} \hbar\omega_{\mathbf{q}} |C_{\mathbf{q}}|^2 |M_{n,\ell,n',\ell'}(\mathbf{q})|^2 \sum_{s=-\infty}^{+\infty} J_s^2\left(\frac{\Lambda}{\hbar\Omega}\right) N_{\mathbf{q}}(T) \\ &\times \left\{ \left[f_{n,\ell,k_z}(T_e) - f_{n',\ell',k_z+q_z}(T_e) \right] \right. \\ &\times \delta\left(E_{n,\ell}(k_z) - E_{n',\ell'}(k_z+q_z)) + \hbar\omega_{\mathbf{q}} + s\hbar\Omega \right) \\ &- \left[f_{n,\ell,k_z}(T_e) - f_{n',\ell',k_z-q_z}(T_e) \right] \\ &\times \left. \delta\left(E_{n,\ell}(k_z) - E_{n',\ell'}(k_z-q_z)) - \hbar\omega_{\mathbf{q}} - s\hbar\Omega \right) \right\}. \end{aligned} \tag{10}$$

We can see that in a situation where the electrons temperature T_e equals to the phonons temperature T, the cooling power vanishes as required by detailed balance between the absorption and emission processes. At $T = 0$, where there are no thermally excited phonons, the second term in Eq. (9) equals to zero and the cooling power is given entirely by spontaneous emission processes (Kaasbjerg et al. 2014). The expression for the cooling power obtained here is general and can be applied to any kinds of phonon as well as a general electronic band structure.

In this calculation, we assume that electrons emit/absorb only optical phonons at high temperatures. Also, optical phonons are assumed to be dispersionless, i. e., $\omega_{\mathbf{q}} \approx \omega_0 =$ constant. In this case (Bau and Phong 1998), $|C_{\mathbf{q}}|^2 = e^2\hbar\omega_0\left(\chi_\infty^{-1} - \chi_0^{-1}\right)/(2\epsilon_0 V_0 q^2)$ where V_0, ϵ_0, χ_0 and χ_∞ are the normalisation volume, the electronic constant, the static and the high-frequency dielectric constant, respectively. To obtain an explicit expression for $F(T)$ from Eq. (10), we transform the summations with respect to k_z and q to integrals as $(L/2\pi)\int_0^\infty dk_z$, $V_0/(2\pi)^2\int_0^\infty q_\perp dq_\perp \int_0^\infty dq_z$, also we consider only the Bessel functions with $s = -1, 0, 1$. After a straight-forward calculation, we have

$$F(T) = F_1 + F_2 + F_3 + F_4 + F_5 + F_6, \tag{11}$$

where

$$\begin{aligned}
F_1 =& \frac{\omega_0 e^4 L E_0^2}{64\pi^2 \Omega^4 m_\mathrm{e} \hbar^4 \epsilon_0}\Big(\frac{1}{\chi_\infty}-\frac{1}{\chi_0}\Big)\sum_{n,\ell,n',\ell'} \hbar\omega_0 N_\mathbf{q}(T) H_{n,\ell,n',\ell'} \exp\Big[\frac{1}{k_\mathrm{B}T_\mathrm{e}}\Big(E_\mathrm{F}-\frac{\hbar^2 x_{n,\ell}^2}{2m_\mathrm{e}R^2}\Big)\Big] \\
&\times\Big[\exp\Big(\frac{C_{+|s=1}}{2k_\mathrm{B}T_\mathrm{e}}\Big)K_0\Big(\frac{C_{+|s=1}}{2k_\mathrm{B}T_\mathrm{e}}\Big)-\exp\Big(\frac{C_{-|s=1}}{2k_\mathrm{B}T_\mathrm{e}}\Big)K_0\Big(\frac{C_{-|s=1}}{2k_\mathrm{B}T_\mathrm{e}}\Big)\Big], \\
F_2 =& \frac{\omega_0 e^2 L m_\mathrm{e}}{16\pi^2 \hbar^2 \epsilon_0}\Big(\frac{1}{\chi_\infty}-\frac{1}{\chi_0}\Big)\sum_{n,\ell,n',\ell'} \hbar\omega_0 N_\mathbf{q}(T) H_{n,\ell,n',\ell'} \exp\Big[\frac{1}{k_\mathrm{B}T_\mathrm{e}}\Big(E_\mathrm{F}-\frac{\hbar^2 x_{n,\ell}^2}{2m_\mathrm{e}R^2}\Big)\Big] \\
&\times\Big[\Big(\frac{2m_\mathrm{e}C_{+|s=0}}{\hbar^2}\Big)^{-1}\exp\Big(\frac{C_{+|s=0}}{2k_\mathrm{B}T_\mathrm{e}}\Big)K_{-1}\Big(\frac{C_{+|s=0}}{2k_\mathrm{B}T_\mathrm{e}}\Big) \\
&-\Big(\frac{2m_\mathrm{e}C_{-|s=0}}{\hbar^2}\Big)^{-1}\exp\Big(\frac{C_{-|s=0}}{2k_\mathrm{B}T_\mathrm{e}}\Big)K_{-1}\Big(\frac{C_{-|s=0}}{2k_\mathrm{B}T_\mathrm{e}}\Big)\Big], \\
&-\frac{1}{2}\Big(\frac{eE_0}{m_\mathrm{e}\hbar\Omega^2}\Big)^2\Big[\exp\Big(\frac{C_{+|s=0}}{2k_\mathrm{B}T_\mathrm{e}}\Big)K_0\Big(\frac{C_{+|s=0}}{2k_\mathrm{B}T_\mathrm{e}}\Big)-\exp\Big(\frac{C_{-|s=0}}{2k_\mathrm{B}T_\mathrm{e}}\Big)K_0\Big(\frac{C_{-|s=0}}{2k_\mathrm{B}T_\mathrm{e}}\Big)\Big], \\
F_3 =& \frac{\omega_0 \Omega^4 L m_\mathrm{e}^3}{4\pi^2 E_0^2 \epsilon_0}\Big(\frac{1}{\chi_\infty}-\frac{1}{\chi_0}\Big)\sum_{n,\ell,n',\ell'} \hbar\omega_0 N_\mathbf{q}(T) H_{n,\ell,n',\ell'} \exp\Big[\frac{1}{k_\mathrm{B}T_\mathrm{e}}\Big(E_\mathrm{F}-\frac{\hbar^2 x_{n,\ell}^2}{2m_\mathrm{e}R^2}\Big)\Big] \\
&\times\Big[\Big(\frac{2m_\mathrm{e}C_{+|s=-1}}{\hbar^2}\Big)^{-2}\exp\Big(\frac{C_{+|s=-1}}{2k_\mathrm{B}T_\mathrm{e}}\Big)K_{-2}\Big(\frac{C_{+|s=-1}}{2k_\mathrm{B}T_\mathrm{e}}\Big) \\
&-\Big(\frac{2m_\mathrm{e}C_{-|s=-1}}{\hbar^2}\Big)^{-2}\exp\Big(\frac{C_{-|s=-1}}{2k_\mathrm{B}T_\mathrm{e}}\Big)K_{-2}\Big(\frac{C_{-|s=-1}}{2k_\mathrm{B}T_\mathrm{e}}\Big)\Big], \\
F_4 =& \frac{\omega_0 e^4 L E_0^2}{64\pi^2 \Omega^4 m_\mathrm{e} \hbar^4 \epsilon_0}\Big(\frac{1}{\chi_\infty}-\frac{1}{\chi_0}\Big)\sum_{n,\ell,n',\ell'} \hbar\omega_0 N_\mathbf{q}(T) H_{n,\ell,n',\ell'} \exp\Big[\frac{1}{k_\mathrm{B}T_\mathrm{e}}\Big(E_\mathrm{F}-\frac{\hbar^2 x_{n',\ell'}^2}{2m_\mathrm{e}R^2}\Big)\Big] \\
&\times\Big[\exp\Big(\frac{-C_{-|s=1}}{2k_\mathrm{B}T_\mathrm{e}}\Big)K_0\Big(\frac{C_{-|s=1}}{2k_\mathrm{B}T_\mathrm{e}}\Big)-\exp\Big(\frac{-C_{+|s=1}}{2k_\mathrm{B}T_\mathrm{e}}\Big)K_0\Big(\frac{C_{+|s=1}}{2k_\mathrm{B}T_\mathrm{e}}\Big)\Big], \\
F_5 =& \frac{\omega_0 e^2 L m_\mathrm{e}}{16\pi^2 \hbar^2 \epsilon_0}\Big(\frac{1}{\chi_\infty}-\frac{1}{\chi_0}\Big)\sum_{n,\ell,n',\ell'} \hbar\omega_0 N_\mathbf{q}(T) H_{n,\ell,n',\ell'} \exp\Big[\frac{1}{k_\mathrm{B}T_\mathrm{e}}\Big(E_\mathrm{F}-\frac{\hbar^2 x_{n',\ell'}^2}{2m_\mathrm{e}R^2}\Big)\Big] \\
&\times\Big[\Big(\frac{2m_\mathrm{e}C_{-|s=0}}{\hbar^2}\Big)^{-1}\exp\Big(\frac{-C_{-|s=0}}{2k_\mathrm{B}T_\mathrm{e}}\Big)K_{-1}\Big(\frac{C_{-|s=0}}{2k_\mathrm{B}T_\mathrm{e}}\Big) \\
&-\Big(\frac{2m_\mathrm{e}C_{+|s=0}}{\hbar^2}\Big)^{-1}\exp\Big(\frac{-C_{+|s=0}}{2k_\mathrm{B}T_\mathrm{e}}\Big)K_{-1}\Big(\frac{C_{+|s=0}}{2k_\mathrm{B}T_\mathrm{e}}\Big)\Big], \\
&-\frac{1}{2}\Big(\frac{eE_0}{m_\mathrm{e}\hbar\Omega^2}\Big)^2\Big[\exp\Big(\frac{-C_{-|s=0}}{2k_\mathrm{B}T_\mathrm{e}}\Big)K_0\Big(\frac{C_{-|s=0}}{2k_\mathrm{B}T_\mathrm{e}}\Big)-\exp\Big(\frac{-C_{+|s=0}}{2k_\mathrm{B}T_\mathrm{e}}\Big)K_0\Big(\frac{C_{+|s=0}}{2k_\mathrm{B}T_\mathrm{e}}\Big)\Big], \\
F_6 =& \frac{\omega_0 \Omega^4 L m_\mathrm{e}^3}{4\pi^2 E_0^2 \epsilon_0}\Big(\frac{1}{\chi_\infty}-\frac{1}{\chi_0}\Big)\sum_{n,\ell,n',\ell'} \hbar\omega_0 N_\mathbf{q}(T) H_{n,\ell,n',\ell'} \exp\Big[\frac{1}{k_\mathrm{B}T_\mathrm{e}}\Big(E_\mathrm{F}-\frac{\hbar^2 x_{n',\ell'}^2}{2m_\mathrm{e}R^2}\Big)\Big] \\
&\times\Big[\Big(\frac{2m_\mathrm{e}C_{-|s=-1}}{\hbar^2}\Big)^{-2}\exp\Big(\frac{-C_{-|s=-1}}{2k_\mathrm{B}T_\mathrm{e}}\Big)K_{-2}\Big(\frac{C_{-|s=-1}}{2k_\mathrm{B}T_\mathrm{e}}\Big) \\
&-\Big(\frac{2m_\mathrm{e}C_{+|s=-1}}{\hbar^2}\Big)^{-2}\exp\Big(\frac{-C_{+|s=-1}}{2k_\mathrm{B}T_\mathrm{e}}\Big)K_{-2}\Big(\frac{C_{+|s=-1}}{2k_\mathrm{B}T_\mathrm{e}}\Big)\Big], \qquad (12)
\end{aligned}$$

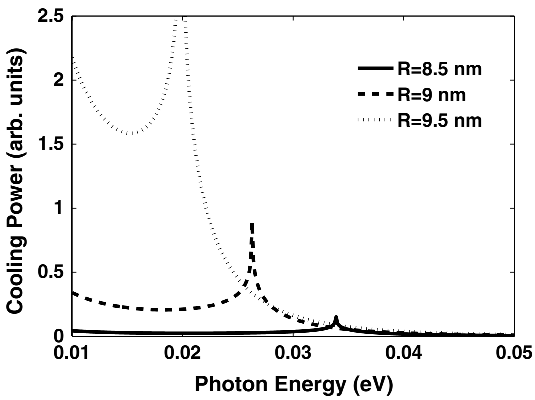

Fig. 1 Dependence of the CP on the photon energy for three different values of the CQW radius. Here, $E_0 = 4 \times 10^5$ V m^{-1}, and $T_e = 77$ K

with E_F being the Fermi energy, k_B being the Boltzmann constant, and

$$H_{n,\ell,n',\ell'} = \int_0^\infty q_\perp |M_{n,\ell,n',\ell'}(q_\perp)|^2 dq_\perp, \tag{13}$$

$$C_{+|s=\pm1} = -\Delta E_{n,\ell,n',\ell'} + \hbar\omega_0 \pm \hbar\Omega, \tag{14}$$

$$C_{-|s=\pm1} = -\Delta E_{n,\ell,n',\ell'} - \hbar\omega_0 \mp \hbar\Omega, \tag{15}$$

$$C_{\pm|s=0} = -\Delta E_{n,\ell,n',\ell'} \pm \hbar\omega_0. \tag{16}$$

Here, we have set $\Delta E_{n,\ell,n',\ell'} = \hbar^2 x^2_{n',\ell'}/(2m_e R^2) - \hbar^2 x^2_{n,\ell}/(2m_e R^2)$. The present result yields a more specific and significant interpretation of the electronic processes for emission and absorption of phonon and photon. These analytical results appear very complicated. However, physical conclusions can be drawn from graphical representations and numerical results, obtained from adequate computational calculations.

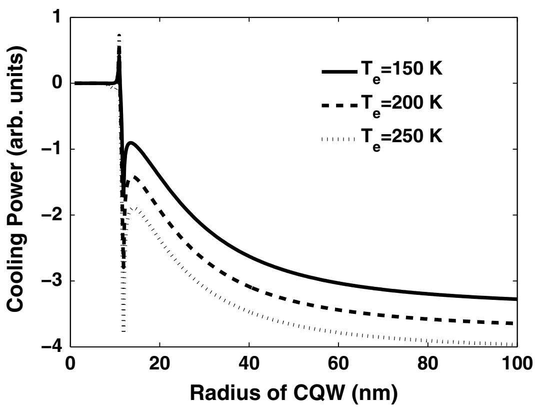

Fig. 2 Dependence of the CP on the radius of CQW for three different values of electron temperature. Here, $E_0 = 4 \times 10^5$ V m^{-1}, and $\omega = 10^{13}$ s^{-1}

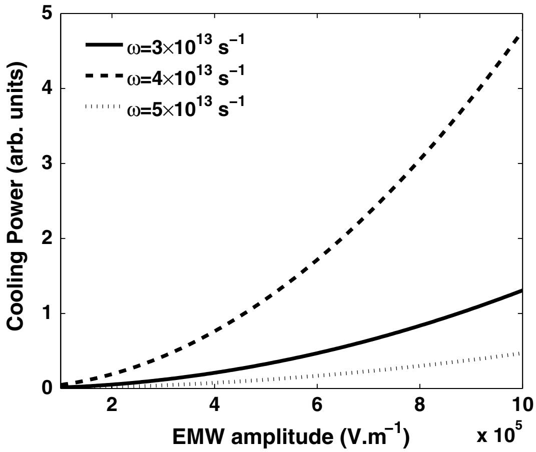

Fig. 3 Dependence of the CP on the EMW amplitude at different values of the EMW frequency. Here, $T_e = 77$ K, and $R = 9$ nm

4 Numerical results and discussion

To clarify physical meanings of the above obtained result, in this section we numerically evaluate the CP using specific parameters of GaAs/AlAs CQW. The parameters taken in the evaluation are as follows (Masale and Constantinou 1993): $\chi_\infty = 10.9$, $\chi_0 = 12.9$, $m_e = 0.067 \times m_0$ (m_0 being the mass of free electron), $\hbar\omega_0 = 36.25$ meV, $E_F = 0.115 \times 10^{-18}$ J. Also, we only consider the electron transitions between the lowest subbands: $n, n' = 0, 1$; $\ell = \ell' = 1$. By computation, one can obtain $x_{0,1} = 2.4048$, $x_{1,1} = 3.8317$, $y_{0,1} = 0.5192$, $y_{1,1} = 0.4028$. The characteristics are obtained for the lattice temperature $T = 60$ K. The assumption of the extreme quantum limit is satisfied for this choice of parameters.

In Fig. 1, we show the hot electron cooling power as a function of the photon energy at different values of the CQW radius. In general, the CP decreases with increasing the photon energy. Because along with losing energy for phonons, electrons gain the energy from photons so their energy lost rate is smaller than it is in the case of absence of the EMW. From the figure, we also see that the CP reaches maximum at a special value of the photon energy. To deduce the physical meaning of this maximum we examine, as an example, the case of $R = 9$ nm (the dashed curve). In this case, $\Delta E_{0,1,1,1} = 62.5492$ meV and the resonant peak is at the photon energy of 26.2992 meV ($\omega \approx 3.9941 \times 10^{13}$ s^{-1}). Therefore, this resonant peak appears under the condition $\hbar\omega = \Delta E_{0,1,1,1} - \hbar\omega_0$. This condition implies the resonant transition of electrons in the CQW between two subbands $|0, 1\rangle$ and $|1, 1\rangle$ via the emission of an optical phonon with energy $\hbar\omega_0 = 36.25$ meV along with the emission of a photon with the energy of 26.2992 meV. The appearance of the peak on other curves can be explained similarly. In short, electron cooling process here can take place via two channels: transferring energy to phonons and emitting photons. The rate of electron cooling reaches maximum when the energy difference between subbands is equal to the energy of an optical phonon plus photon energy. This behaviour is new in comparison to those obtained in the previous works where the EMW was absent.

Figure 2 shows the electron energy loss rate versus the radius of CQW at the electron temperature of 150, 200, and 250 K and the EMW frequency of 10^{13} s^{-1}. We can see that for small radii of CQW, the CP has positive value, i. e., electrons lose their energy to the phonons system. As the radius increases, the CP changes its sign and is always negative. A negative CP means that electrons in the system can gain the energy from the corresponding electronic transitions induced by absorbing optical phonon and/or photon. Moreover, for extremely large radii, the CP varies not considerably.

The effect of the EMW amplitude on the CP is shown in Fig. 3 where we plot the CP versus the EMW amplitude at different values of the EMW frequency. It can be seen from the figure that the CP increases with increasing the EMW amplitude. This can be explained as follows. As the EMW amplitude increases, i.e., the intensity of the EMW increases, the energy that the electrons system receives from the EMW per time unit should increases. Therefore, the energy transfer rate from electrons to phonons must increase so that the electron temperature remains constant (77 K in this case) instead of heating up. In addition, we can see that the CP is largest for the EMW frequency of 4×10^{13} s^{-1}, this value is close to the value that satisfies the condition $\hbar\omega = \Delta E_{0,1,1,1} - \hbar\omega_0$ as shown in Fig. 1.

5 Conclusions

So far, we have investigated the hot electron cooling by phonons in CQWs in the presence of an EMW. The hot electron CP has been derived for the case of electron–optical phonon interaction. The results show that there exists resonant behaviour in the photon energy (frequency) dependence of the CP. The CP reaches maximum value when a resonant scattering happens in the electron–phonon–photon system where an electron transits between its subband levels by emitting an optical phonon and a photon. The negative CP implies that electrons gain energy from phonon and photon instead of losing their energy. In addition, the CP at fixed temperatures and CQW radius increases when the EMW amplitude increases.

References

Balkan, N. (ed.): Hot Electrons in Semiconductors: Physics and Devices. Oxford University Press, Oxford (1998)

Bau, N.Q., Phong, T.C.: Calculations of the absorption coefficient of a weak electromagnetic wave by free carriers in quantum wells by the Kubo–Mori method. J. Phys. Soc. Jpn. **67**, 3875–3880 (1998)

Betz, A.C.: Hot electron cooling by acoustic phonons in graphene. Phys. Rev. Lett. **109**, 056805–056809 (2012)

Bhargavi, K.S., Kubakaddi, S.S.: High field transport properties of a bilayer graphene. Physica E **56**, 123–129 (2014)

Bhargavi, K.S., Kubakaddi, S.S.: Electron cooling in three-dimensional Dirac fermion systems at low temperature: effect of screening. Phys. Status Solidi Rapid Res. Lett. **10**, 248–252 (2016)

Butler, S.Z.: Progress challenges, and opportunities in two-dimensional materials beyond graphene. ACS Nano **7**(4), 2898–2926 (2013)

Castro Neto, A.H., Guinea, F., Peres, N.M.R., Novoselov, K.S., Geim, A.: The electronic properties of graphene. Rev. Mod. Phys. **81**, 109–162 (2009)

Das Sarma, S., Adam, S., Hwang, E.H., Rossi, E.: Electronic transport in two-dimensional graphene. Rev. Mod. Phys. **83**, 407–470 (2011)

Fletcher, R., Pudalov, V.M., Feng, Y., Tsaousidou, M., Butcher, P.N.: Thermoelectric and hot-electron properties of a silicon inversion layer. Phys. Rev. B **56**, 12422–12428 (1997)

Gaška, R., Mickevičius, R., Mitin, V., Grubin, H.L.: Hot-electron overcooling and intersubband population inversion in quantum wires. Semicond. Sci. Technol. **9**, 886–888 (1994)

Gaška, R., Mickevičius, R., Mitin, V., Stroscio, M.A., Iafrate, G.J., Grubin, H.L.: Hotelectron relaxation dynamics in quantum wires. J. Appl. Phys. **76**, 1021–1028 (1994)

Gupta, A., Sakthivel, T., Seal, S.: Recent development in 2D materials beyond graphene. Prog. Mater. Sci **73**, 44–126 (2015)

Hoi, B.D., Phuong, L.T.T., Phong, T.C.: Magneto-optical absorption and cyclotron–phonon resonance in graphene monolayer. J. Appl. Phys. **123**, 094303 (2018)

Iacopi, F., Boeckl, J.J., Jagadish, C. (ed.): Book Series: Semiconductors and Semimetals, 2D Materials, 95, 2–340 (2016)

Kaasbjerg, K., Bhargavi, K.S., Kubakaddi, S.S.: Hot-electron cooling by acoustic and optical phonons in monolayers of MoS_2 and other transition-metal dichalcogenides. Phys. Rev. B **90**, 165436 (2014)

Kang, N.L., Lee, Y.J., Choi, S.D.: Derivation of the DC conductivity in a quantum well by using an operator algebra technique. J. Korean Phys. Soc. **44**, 1535–1541 (2004)

Kubakaddi, S.S.: Interaction of massless Dirac electrons with acoustic phonons in graphene at low temperatures. Phys. Rev. B **79**, 075417-1–075417-6 (2009)

Kubakaddi, S.S.: Cerenkov emission of acoustic phonons electrically generated from three-dimensional Dirac semimetals. J. Appl. Phys. **119**, 195701 (2016)

Kubakaddi, S.S.: The role of vector potential coupling in hot electron cooling power in bilayer graphene at low temperature. Physica E **95**, 144–148 (2018)

Kubakaddi, S.S., Suresha, K., Mulimani, B.G.: Energy loss rate of two-dimensional electron gas in GaInAs/AlInAs, InSb/AlInSb and GaSb/AlGaAsSb heterostructures. Physica E **18**, 475–484 (2003)

Lee, S.-C., Galbraith, I., Pidgeon, C.R.: Influence of electron temperature and carrier concentration on electron-LO-phonon intersubband scattering in wide GaAs/$Al_xGa_{1-x}As$ quantum wells. Phys. Rev. B **52**, 1874–1881 (1995)

Ma, Y., Fletcher, R., Zaremba, E., D'lorio, M., Foxon, C.T., Harris, J.J.: Energy-loss rates of two-dimensional electrons at a GaAs/$Al_xGa_{1-x}As$ interface. Phys. Rev. B **43**, 9033–9044 (1991)

Masale, M., Constantinou, N.C.: ElectronLO-phonon scattering rates in a cylindrical quantum wire with an axial magnetic field: analytic results. Phys. Rev. B **48**, 11128–11134 (1993)

Mitin, V.V., Gaška, R., Mickevičius, R.: Ultrafast relaxation of hot electrons in quantum wires. In: Proceedings of SPIE 2142, Ultrafast Phenomena in Semiconductors, 69 (May 6, 1994), https://doi.org/10.1117/12.175911

Mori, N., Ando, T.: Magnetophonon resonance in monolayer graphene. J. Phys. Soc. Jpn. **80**, 044706 (2011)

Nguyen, C.V.: Magneto-optical transport properties of monolayer MoS2 on polar substrates. Phys. Rev. B **96**, 125411 (2017)

Qu, S.-X., Cleland, A.N., Geller, M.R.: Hot electrons in low-dimensional phonon systems. Phys. Rev. B **72**, 224301-1–224301-7 (2005)

Sangwan, V.K., Hersam, M.C.: Electronic transport in two-dimensional materials. Annu. Rev. Phys. Chem. **69**, 299–325 (2018)

Shadrin, V.D., Kistenev, F.E., Serzhenko, F.L.: Influence of quantum wire electron confinement on intrasubband polaroptical scattering rates. J. Appl. Phys. **75**, 985–988 (1994)

Sippel, P.: Femtosecond cooling of hot electrons in CdSe quantum-well platelets. Nano Lett. **15**, 2409–2416 (2015)

Smith, H., Jensen, H.H.: Transport Phenomena. Oxford University Press, Oxford (1989)

Stange, A., Sohrt, C., Yang, L.X., Rohde, G., Janssen, K., Hein, P., Oloff, L.-P., Hanff, K., Rossnagel, K., Bauer, M.: Hot electron cooling in graphite: supercollision versus hot phonon decay. Phys. Rev. B **92**, 184303 (2015)

Stroscio, M.A., Dutta, M.: Phonons in Nanostructures. Cambridge University Press, Cambridge (2001)

Wang, X.F., Lei, X.L.: Polar-optic phonons and high-field electron transport in cylindrical GaAs/AlAs quantum wires. Phys. Rev. B **49**(7), 4780–4789 (1994)

Xu, W.: Emission of acoustic and optical phonons by hot electrons in a two-dimensional electron system in parallel magnetic fields. Phys. Rev. B **54**, 2775–2784 (1996)

Xu, W., Dong, H.M., Li, L.L., Yao, J.Q., Vasilopoulos, P., Peeters, F.M.: Optoelectronic properties of graphene in the presence of optical phonon scattering. Phys. Rev. B **82**, 125304–125309 (2010)

Yarmohammadi, M.: Strain effects on the optical conductivity of gapped graphene in the presence of Holstein phonons beyond the Dirac cone approximation. AIP Adv. **6**(8), 085008 (2016)

Yarmohammadi, M.: Thermodynamic properties of gapped graphene in the presence of a transverse magnetic field by considering holstein phonons. J. Electron. Matter. **46**(2), 747–757 (2017a)

Yarmohammadi, M.: The electronic properties, electronic heat capacity and magnetic susceptibility of monolayer boron nitride graphene-like structure in the presence of electron–phonon coupling. Solid State Commun. **253**, 57–62 (2017b)

Yarmohammadi, M., Mirabbaszadeh, K., Shirzadi, B.: The effects of Rashba spinorbit coupling and Holstein phonons on thermodynamic properties of BN-doped graphene. Int. J. Mod. Phys. B **31**(8), 1750045 (2017)